Effects of high-fat diet on the epithelial-mesenchymal transition of respiratory tract through the glyoxylic acid cycle of pulmonary microbes and the intervention of saturated hydrogen

Xiangjie Qiu
Central South University Xiangya School of Medicine
Ousman Bajinka
Central South University Xiangya School of Medicine
Lili Wang
Central South University Xiangya School of Medicine
Guojun Wu
Central South University Xiangya School of Medicine
Yurong Tan (yurongtan@csu.edu.cn)
Central South University https://orcid.org/0000-0002-2871-4078

Research

Keywords: high-fat diet, pulmonary microecology, glyoxylic acid cycle, epithelial-mesenchymal transition, saturated hydrogen

Posted Date: March 17th, 2020

DOI: https://doi.org/10.21203/rs.3.rs-17519/v1

Abstract

Background High fat diet is extensively studied to be associated with trending metabolic diseases. In addition to type 2 diabetes and hypertension, high fat diet is strongly associated with asthma and other respiratory diseases among children however, the pathogenicity regarding these pulmonary diseases begs for extensive research. This study investigated the mechanism of the epithelial-mesenchymal transition of respiratory tract, induced by changes in lung microecology with the intake of high-fat diet. 80 five-week-old C57BL6/J male mice were randomly divided into normal control group, normal hydrogen group, high-fat group and high-fat hydrogen group, making 20 mice in each group. The weight of the mice were measured on weekly basis. 6 mice from each group were executed at every second week. Blood sample was collected for lipid testing, lung tissues were collected for 16SrRNA gene sequencing, HE staining, immunofluorescence and quantitative real-time PCR (qPCR).

Results Compared with the normal diet group, mice on the high-fat diet group showed increased inflammatory cell infiltration, decreased expression of e-cadherin (E-cad) and increased expression of Twist. There were significant differences in the composition of bacteria in the lung, and the expression of isocitrate lyase (ICL) gene in Pseudomonas aeruginosa , Staphylococcus aureus and Acinetobacter baumannii , which were significantly associated with asthma were seen with a significant increasing trend. After the treatment of saturated hydrogen, the changes in lung microbial population, lung tissue infiltration of inflammatory cells and the transformation of epithelial stroma caused by high-fat diet were moderately alleviated.

Conclusion High fat diet can affect the process of airway epithelial stroma by altering the glyoxylate cycle of pulmonary microbes while the pathological process are alleviated by saturated hydrogen by acting on glyoxylate cycle.

Introduction

High fat diet is not only associated with type 2 diabetes (T2DM), hypertension and other metabolic diseases, but is also studied to be correlating significantly with asthma and other respiratory diseases. Based on the previous studies, the incidence of asthma and asthmatic diseases in children with high-fat diet is significantly higher than children without high-fat diet [1, 2] however, the pathogenicity underpinning high-fat diet with asthma is still in the mystery. Asthma is a chronic airway inflammatory disease, which often occurs with airway remodeling [3, 4]. Airway remodeling is based on chronic airway inflammation, which leads to the irreversible changes of airway structure. Subepithelial fibrosis is one of the core characteristics of airway remodeling, which is associated with the severity of asthma and one of the main causes of death in patients with severe asthma [5, 6]. Airway epithelial mesenchymal transition (EMT) is a cell biological process in which epithelial cells are transformed into stromal phenotypes through a specific process, which plays an important role in airway remodeling of asthma. Airway remodeling can improve the degree of subepithelial fibrosis of airway through EMT [7]. Early prevention

and treatment of airway remodeling and reduction of fibrosis in asthmatic patients is an intervention that do not only control the level of asthma but also enhance the prognosis.

Modern day science is blessed with 16SrRNA gene sequencing technology that enhanced microbial characterization and ascertained more than 30 bacterial species planted in the lungs [8]. Going by the published studies, the diversity of microbes in the lung is biological imperative in maintaining the normal airway function, and in addition to bacterial, fungi and viruses constitute the intrapulmonary microecology. Studies based on common respiratory diseases, alteration or changes in the diversity of microbes are associated with asthma and pulmonary fibrosis [9–11]. A number of studies meet a consensus that in respiratory diseases such as asthma and chronic obstructive pulmonary diseases (COPD), abnormal increase in abundance of species such as Pseudomonas aeruginosa, Acinetobacter baumannii, Staphylococcus aureus, Klebsiella pneumoniae, and Haemophilus influenzae was observed [12, 13].

The glyoxylic acid cycle is a metabolic pathway in prokaryotes, lower eukaryotes, and plants, and it is essential for the energy metabolism. Studies have shown that the glyoxylate cycle also exists in many opportunistic pathogens. These opportunistic pathogens use the host's fatty acid degradation products to synthesize substances required for their normal growth and reproduction, split macrophages from the inside, and then expand in abundance in the host [14]. Fatty acids are decomposed into acetyl-CoA by beta-oxidation, which form citric acid with oxaloacetate produced from two acetates through the glyoxylic cycle. Under the action of aconitase, citric acid produces isocitrate, which is broken by isocitrate lyase (ICL) to produce glyoxylic acid and succinic acid. Next, glyoxylic acid and acetyl-CoA produce malic acid under the catalysis of malic acid synthetase and malic acid is dehydrogenated to oxaloacetic acid under the catalysis of malic acid dehydrogenase. The succinic acid produced in this cycle can be used to synthesize sugars and other cellular components, which defined ICL as the most critical enzyme in the glyoxylic acid cycle [15].

Number of studies have shown that viral infection and high-fat diet can lead to the accumulation of fatty acids in cells. Therefore, we speculate that the high-fat airway microenvironment caused by high-fat diet leads to an imbalance of airway microecology through the promotion of the glyoxylate cycle of microbes. We further hypothesized that the abnormal increase of opportunistic pathogens mediate chronic airway inflammation, thus promoting the occurrence of asthma and airway remodeling.

Hydrogen (H_2) has antioxidant, anti-inflammatory, and anti-apoptotic properties and is the most abundant chemical element in the world [16]. In 2007, Ohsawa et al [17] confirmed that inhaling 2% hydrogen could lead to selective scavenging of hydroxyl radicals (OH) and peroxynitrite anions ($ONOO^-$), which significantly enhance cerebral ischemia-reperfusion injury in rats. After long-term drinking of hydrogen-rich water by obese mice with T2DM, liver malondialdehyde level, fat content, blood sugar, and blood total glyceride (TG) levels all decreased [18, 19], suggesting that hydrogen could improve metabolic disorders of lipids and glucose, as well as the metabolic syndrome. Therefore, we use saturated hydrogen as a

treatment factor to explore whether it can improve the effect of lipid metabolism disorder caused by high-fat diet on the transformation of respiratory epithelial stroma.

Results

The mice on the high-fat diet show significant increase in body weights and dyslipidemia, which was aborogated by saturated hydrogen.

As shown in Figure 1A, the average weight of mice in the HF+H_2 group on the 42nd day was 34.05 ± 2.15 g, 20% higher than that of mice in the Control group, which was 27.45 ± 1.15 g, meaning that the average weight of mice in the HF+H_2 group meet the weight standard of obese mice. The average weights of mice in the H_2 and HF+H_2 groups decreased after treatment with saturated hydrogen when compared with those in the corresponding Control and HF groups, as shown in Figure 1B, indicating that saturated hydrogen inhibited the increase in body weights of mice.

On day 28, total cholesterol (TC) and low-density lipoprotein (LDL) in the HF group increased significantly compared with those in the Control group, and LDL in the HF+H_2 group decreased considerably compared with the HF group (Figure 1 C, E). On day 42, TG, TC, and LDL in the HF group increased markedly compared with those in the Control group, which decreased substantially after saturated hydrogen treatment (Figure 1C, D, and E). However, high-density lipoprotein (HDL) in the HF group decreased remarkably compared with the Control group, and it increased dramatically in the HF+H_2 group compared with the HF group (Figure 1F), suggesting that saturated hydrogen reduces TC, TG, and LDL levels and increases the content of HDL in the peripheral blood of obese mice.

In the high-fat diet group, the infiltration of inflammatory cells in the lung tissues increased and EMT increased.

It can be seen from the HE staining results of the lung histopathological sections (Figure 2A) that after day 42 on high-fat diet, the infiltration degree of inflammatory cells around the bronchus in HF group increased compared with that of the Control group, with a small amount of inflammatory cells infiltrating in the lumens and a little shedding of bronchial cilia. Compared with the HF group, the pathological changes were decreased in the HF+H_2 group. The results of qPCR showed that the expression of E-cadherin was significantly decreased and twist was significantly increased in the HF group compared with the Control group. Compared with the HF group, the expression of E-cadherin gene in the HF+H_2 group increased, and twist decreased, but there was no significant statistical difference (Figure 2B). The results of immunofluorescence showed that the expression of E-cadherin protein decreased significantly at day 42, while the expression of twist protein increased significantly in the HF group compared with the Control group, which was in consistent with the results of qPCR (Figure 2 C, D). These results have shown that high-fat diet can lead to inflammation of lung tissue and accelerate the process of EMT of respiratory tract.

The normal diet group and the high-fat diet group show significant differences in the number and composition of microbes in the lungs.

After the question sequence is eliminated, the total sequencing quantity is 559453. The length distribution of the sequence contained in all samples was statistically analyzed in R software, and the sequence length was mainly distributed between 250-450bp (Supplementary figure 1). Operational taxonomic unit (OTU) whose abundance value was less than 0.001% (1/100,000) of the total sequencing amount of all samples was removed, and the distribution of the remaining OTU in each group is shown as (Figure 3A, Supplementary figure 2). The results showed that the number of OTU on the HF group was significantly higher than that of the Control group at the level of phylum, class, order, genus and species. The analysis of the same OTU between the groups showed that the number of unique OTU in the HF group increased significantly compared with that of the Control group, and the number of unique OTU in the Control and HF groups all decreased after hydrogen administration (Figure 3B). According to the OTU classification and classification status, the specific composition of each sample at the level of phylum, class, order, family, genus and species classification was obtained. The results showed that the number of bacteria in the lung of mice in the HF group was significantly higher than those in the Control group, and there was no significant difference between the hydrogen group and the non-hydrogen group (Figure 3C, D).

The diversity and difference of microflora in the lung of each group.

The rarefaction sparse curve (Chao1), speccaccum species accumulation curve and abundance level curve in alpha diversity analysis tend to be gentle, indicating that the sequencing depth is enough to reflect the diversity and richness of the microbial community contained in the community sample, and the total number of OTUs in the community will no longer increase by significant. With the addition of new samples, and the abundance difference among OTUs in the community, the difference is small and the community composition is high (Figure 4A). According to the alpha diversity index (Chao1, ACE, Shannon, Simpson) (Figure 4B), the diversity of bacteria in the lung of mice in the high fat diet group was significantly higher than that of the normal diet group, and the diversity of mice in the normal hydrogen feeding group was lower than that of the normal control group.

Discriminant analysis by PLS-DA partial least squares and beta diversity based on weighted UniFrac NMDS UPGMA cluster analysis chart of UniFrac distance matrix (Figure 4C) shows that there are obvious differences in the structure of microbial community in the lung of the HF group compared with the Control group, and also some differences in the hydrogen feeding group compared with the non-hydrogen feeding group, and the difference of each mouse within the same group is small. The results show that the animal classification model is effective.

Identification of key microbes with significant difference in pulmonary microflora of mice in each group.

Using R software, cluster analysis and heat map (Figure 5A) were made for the first 50 genera of abundance, which showed that there were significant differences between the high-fat diet group and the

normal diet group, and there were also some differences between the hydrogen group and the non-hydrogen group.

Compared with the Control group, the abundance of the common opportunistic pathogens *Acinetobacter*, *Pseudomonas*, *Corynebacterium*, *Strepcoccus*, *Clostridium*, *Haemophilus* and *Porphyromonas* increased significantly in the HF group. After hydrogen administration, the abundance of *Acinetobacter*, *Clostridium* and *Porphyromonas* decreased significantly. There was a significant decrease in *Bifidobacterium* in the HF group compared with that of the Control group (Figure 5B, C). These results showed that high-fat diet significantly alters the diversity of microbes in the lung of mice, opportunistic pathogens increased while probiotic microbes decreased, thus increased susceptibility of respiratory inflammation.

Functional prediction of bacterial metabolism

The 16S rRNA gene sequence was predicted in KEGG, COG and rfam3 functional spectrum databases by PICRUSt functional prediction analysis. The predicted functional spectrum data are clustered according to the abundance distribution of functional groups or the similarity between samples, and the functional groups and samples are sorted according to the clustering results. Using R software, the functional groups in the top 50 of the abundance were clustered and analyzed, and a heat map (Figure 6A) was drawn, showing that there were significant differences between the high-fat diet group and the normal diet group. R software was used to calculate the number of common functional groups of each sample, and the proportion of common and unique functional groups of each sample was visualized through Venn diagram. The results showed that the number of functional groups in the HF group was significantly increased compared with the Control group, and that in the hydrogen group was decreased compared with the non-hydrogen group (Figure 6B).

Violin diagram was drawn to show the abundance distribution of the predicted functional groups in each sample (Figure 6C). The results showed that the flora abundance of the HF group involved in lipid metabolism, energy metabolism and amino acid metabolism was significantly increased compared with the Control group, while the flora abundance of the HF group involved in glycan biosynthesis, metabolism and glucose metabolism was decreased. The abundance of bacteria involved in cell communication, cell migration, cell growth and death increased significantly. The number of bacteria involved in the transcription of genetic information increased and the abundance of bacteria involved in translation decreased significantly. The abundance of bacteria involved in neurodegenerative diseases and cardiovascular diseases increased significantly. The abundance of bacteria involved in the body's immune system decreased significantly and the abundance of bacteria involved in the endocrine system and circulatory system increased significantly.

The expression of ICL gene in *P. aeruginosa*, *S. aureus*, *A. baumannii*, *K.pneumoniae*, *C. albicans* and *X. maltophilia*

To investigate whether changes in microbes in the lungs of mice on a high-fat diet were due to changes in glyoxylic acid circulation in bacteria caused by a high-fat environment. We designed primers using the

ICL sequence, a key enzyme in the glyoxylic acid cycle, to detect the expression of ICL genes in several clinical pathogens significantly associated with the development of asthma. qPCR results (Figure 7) showed that the ICL gene expression in *P. aeruginosa*, *S. aureus* and *A. baumandii* in the HF group was significantly increased compared with that of the Control group, and *P. aeruginosa* was significantly decreased after hydrogen supplementation. However, *K. pneumoniae*, *C. albicans* and *X. maltophilia* showed no significant changes.

Discussion

The diversity of microbes found in the lung is imperative to maintaining the normal airway function. Our results show that high-fat diet can change the number and microbial species in the lung, some opportunistic pathogens that are significantly associated with the occurrence of respiratory diseases are increasingly abundant, while the abundance of Bifidobacterium is reduced. These increased opportunistic pathogens are believed to mediate the occurrence of chronic airway inflammation, airway hyperresponsiveness and other pathological changes. The results obtain from qPCR and immunofluorescence also showed a significant reduction in the expression of E-cad, a gene related to the epithelial stromal transformation, while the expression of twist was significantly increased in the HF group when compared with the Control group. This indicates that high-fat diet accelerated the process of the epithelial stromal transformation of the respiratory tract, which may affect the occurrence of airway remodeling.

Although we could not establish a correlating result from a similar study, there are couple of studies on obesity related high-fat diet and one such concluded that TH2 immune response and immunopathologic characteristics in murine model of eosinophilic oesophagitis was worsen severely due to high-fat diet [21]. Furthermore, maternal diet enriched with high-fat is studied to be associated with impaired fetal lung development [22].

Both bacteria and fungi can use glyoxylic acid cycle to synthesize their own pathogenic substances, which can survive in macrophages for a long period of time and expand in the host. It has been shown that many pathogenic and opportunistic microbes express isocitrate lyase and start glyoxylate cycle. In the process of infection, P. aeruginosa can activate glyoxylate cycle as an energy metabolism pathway, make it survive in macrophages and spread in large quantities [23]. Glyoxylate cycle is also the main pathway of material and energy metabolism of A. baumannii in macrophages. A. baumannii enters the host via respiratory tract, connects laminin and fibronectin via sialic acid, and enters macrophages via multiple auxiliary receptors on the surface of the host cell [24, 25]. In macrophages, A. baumannii can start the glyoxylate cycle as an energy metabolism pathway to synthesize its own pathogenic substances [26]. C. albicans, a human opportunistic pathogenic fungus, is engulfed by macrophages to form phagocytes at the early stage of infection. Through glyoxylic acid cycle, it uses fatty acids as energy source, and synthesizes its own virulent factor to split macrophages from the inside, and expand in the host [27].

Therefore, in order to investigate whether the changes of microbes in the lung during high-fat diet are related to glyoxylate cycle, we detected the expression of ICL gene of several conditional pathogens intensively related to respiratory diseases. The results showed that the ICL gene of P. aeruginosa, S. aureus and A. baumannii in the lungs of mice fed with high-fat diet had abnormal high expression. The high-fat diet changed the glyoxylate cycle of these pathogenic bacteria in the lung, and the speed in utilizing fatty acids to synthesize the substances needed for self-metabolism and pathogenic substances was accelerated, resulting in the increase abundance of these opportunistic pathogens. However, we did not find any significant changes in ICL of fungi, and we speculated that this may be associated with the antagonistic effect of bacteria on fungi.

Our results also showed that saturated hydrogen treatment could inhibit the growth and expansion of opportunistic pathogens in the lung and the increase ICL gene expression in S. aureus. Therefore, we speculate that saturated hydrogen can regulate the bacterial flora in the lung by acting on the glyoxylate cycle of the microbes and improve the epithelial stromal transformation caused by high-fat diet. However, we recommend further in vitro and in vivo studies to validate our findings.

Conclusion

This study found that the high-fat airway microenvironment caused by high-fat diet can change the abundance of respiratory tract microbes via glyoxylic acid cycle, thus affecting the process of epithelial stromal transformation and the occurrence of respiratory diseases. Saturated hydrogen is highly recommended based on our study as a new substance for improving respiratory diseases. In the annals of prevention and treatment of respiratory infections and diseases, this study provides new ideas and research basis as a new therapeutic approach.

Methods

Animal grouping

A litter of five-week-old C57BL6/J male mice weighing 16-20 g (purchased from Hunan Tianqin Biological Technology Co., Ltd.) were acclimatized for a week during 12hrs of a light/dark cycle at a constant temperature of 25°C and supplied with sterile water (once a day). The mice were randomized into normal control (Control or A), saturated hydrogen (H_2 or B), high-fat (HF or C), and saturated hydrogen + high-fat (HF+H_2 or D) groups (n = 20 each). Control and H_2 group mice were fed with sterile water and low-fat control feed, while HF and H_2+HF group animals were given sterile water and 60% high-fat model feed (purchased from Nantong Trophy Feed Technology Co., Ltd.). Additionally, mice in the Control and HF groups were given 0.5 ml of saline intragastrically once a day, and those in the H_2 and HF+H_2 groups were given 0.5 ml of saturated hydrogen saline once a day. Saturated hydrogen saline was prepared at the Center of Modern Analysis and Detection of Central South University by dissolving molecular hydrogen into normal saline at high pressure (13.5 Mpa). The formulated saturated hydrogen solution was freshly prepared once every week and stored in aluminum packaging to ensure the hydrogen

concentration remained > 0.6 mmol/L. The weights of the mice were taken once in a week. Six mice from each group were sacrificed in the 2nd, 4th, and 6th weeks from the onset of the experiment. Blood, and lung tissues were collected for subsequent analyses. This study was conducted according to the Declaration of Helsinki and approved by the Medical Ethical Committee of the Xiangya School of Medicine. The same experiments were repeated 3 times.

Monitoring body weight and TC, TG, LDL, and HDL concentrations in peripheral blood

Mice were weighed on days 0, 7, 14, 21, 28, 35, and 42, and the figures in kilogram were recorded appropriately. Blood samples were collected from veins using the eyeball extraction method; 35μl of blood was collected from each mouse for blood lipid tests according to the specific operation steps of blood lipid tester and blood lipid test card (Aikang Biotechnology Co., Ltd., Hangzhou, China).

Hematoxylin-eosin (HE) staining

After anesthetizing mice with ether, lung tissues were excised and rinsed with a 0.9% sodium chloride solution. The resected lung tissues were fixed in a 10% formaldehyde solution for 48hrs, embedded in paraffin, and cut into 4μm-thick sections. The tissue sections were then heated to 60°C for 2hrs, dewaxed with xylene (twice, 15 min each), and dehydrated using an increasing alcohol gradient (75%, 95%, and 100%) for 5 min each. HE staining was performed, and the specimens were observed for pathological morphology under an optical microscope.

Determining the expression of E-cad, N-cad, Slug, Snail, Twist and the ICL gene of *S. aureus*, *P. aeruginosa*, *K. pneumoniae*, *A. baumannii*, *X. maltophilia*, *C. albicans* in the lung tissues using real-time quantitative PCR (qPCR)

Primers were designed using the Primer Premier 5.0 program (Supplementary table 1) and synthesized by Dingguochangsheng Biotechnology Co., Ltd., Beijing, China. Lung tissues were collected from each group of mice, and total RNA was extracted with TRizol. RNA purity was analyzed using a nucleic acid analyzer. cDNA was synthesized by reverse transcription and amplified using a qPCR kit (TansGen Biotech Technology Co., Ltd., Beijing, China) according to the manufacturer's instructions. The reaction mixture consist of 1.5μl cDNA, 12.5μl SYBR Green qPCR Master Mix, 1.5μl each of the forward and reverse primers, and diethylpyrocarbonate (DEPC) water, making a total volume of 25μl. qPCR cycling conditions were: 94°C for 3 min, and 35 cycles of [94°C for 45s, 51°C for 45s, and 72°C for 45s], and the relative mRNA expression was calculated using the $2^{-\triangle\triangle Ct}$ method [20].

Immunofluorescence

Excised lung tissue sections were processed as described above and boiled with 0.01M citrate buffer for antigen retrieval. The tissues were then washed twice with PBS (3 min each), fixed with 4% paraformaldehyde for 5 min, washed with phosphate buffered solution (PBS) again (same condition as the first wash), blocked with normal goat serum for 20 min, and incubated overnight with 5 μl of E-cad

(bs-10009R, BEIJING Bioss Biological Technology Co., Ltd.) or Twist (bs-2441R, BEIJING Bioss Biological Technology Co., Ltd.) rabbit anti-mouse primary antibody in a wet box at 4°C. On the following day, the tissue sections were washed thrice with PBS, incubated with a CY3-conjugated goat anti-rabbit secondary antibody (GB21303, Wuhan Seville Biotechnology Co., Ltd.) at room temperature for 1 h, washed three times with PBS, and counterstained with 4'6-diamidino-2-phenylindole (DAPI) (100 ng/ml) for 10 min. After removing moisture from the tissues, the slides were sealed with an anti-fluorescence quenching agent.

Changes in lung microbiota were detected by 16SrRNA gene sequencing Technology

DNA was extracted from lung tissues of four groups of mice. The extraction quality of DNA was detected by 0.8% agarose gel electrophoresis, and the DNA was quantified by ultraviolet spectrophotometer. Primers were designed with microbial ribosomal RNA as the target and according to the conserved region in the sequence. Sample specific Barcode sequences were added to further PCR amplification of rRNA gene variable regions (single or consecutive multiple) or specific gene fragments. PCR amplification was performed by NEB's Q5 high-fidelity DNA polymerase, and the number of cycles was strictly controlled to keep the number of cycles as low as possible while ensuring the same amplification conditions for the same batch of samples. PCR amplification products were detected by 2% agarose gel electrophoresis, and the target fragments were gelled and recovered using AXYGEN gel recovery kit. Based on the preliminary quantitative results of electrophoresis, fluorescence quantification was performed for the PCR amplification of the recovered products. The fluorescent reagent was the quantit PicoGreen dsDNA Assay Kit and the quantitative instrument was the Microplate reader (BioTek, FLx800). According to the fluorescence quantitative results and the sequencing quantity demand of each sample, the samples were mixed according to the corresponding proportion. Illumina MiSeq sequencing was used as an example to prepare a sequencing Library using Illumina's TruSeq Nano DNA LT Library Prep Kit, and then high-throughput sequencing was performed on the machine. (Detected in Shanghai paisenno Biotechnology Co., Ltd)

Statistical analysis

The SPSS21.0 software was used for statistical analysis, and the data were expressed as mean ± standard deviation. The t-test was used for comparisons between two groups, variance analysis was used for comparisons among multiple groups, and the least significant difference (LSD) was used for comparisons between intra-group differences. P-value < 0.05 was considered statistically significant.

Abbreviations

E-cad
E-cadherin
N-cad
N-cadherin
ICL

Isocitrate lyase
T2DM
Type 2 diabetes
EMT
Epithelial mesenchymal transition
COPD
Chronic obstructive pulmonary diseases
OH
Hydroxyl radicals
$ONOO^-$
Peroxynitrite anions
TG
Total glyceride
TC
Total cholesterol
LDL
Low-density lipoprotein
HDL
High-density lipoprotein
OUT
Operational taxonomic unit
DEPC
Diethylpyrocarbonate
PBS
Phosphate buffered solution
DAPI
4'6-diamidino-2-phenylindole
LSD
Least significant difference

Declarations

Ethics approval and consent to participate

The study was approved by the Institutional Ethic Committee of Xiangya School of Medicine, Central South University.

Consent for publication

Not applicable

Availability of data and materials

The datasets generated during and/or analysed during the current study are available from the corresponding author on reasonable request.

Competing interests

The authors declare that they have no competing interests.

Funding

This work was supported by Grant 31670121 and 31771277 from National Natural Science Foundation of China.

Authors' contributions

QX carried out the study. QX and OB performed the statistical analysis. TY, WG and WL participated in the design of the study. All authors read and approved the submission.

Acknowledgements

Not applicable

References

1. Lin YP, Kao YC, Pan WH, Yang YH, Chen YC, Lee YL. Associations between Respiratory Diseases and Dietary Patterns Derived by Factor Analysis and Reduced Rank Regression. Ann Nutr Metab. 2016;68(4):306-14
2. Patel S, Custovic A, Smith JA, Simpson A, Kerry G, Murray CS. Cross-sectional association of dietary patterns with asthma and atopic sensitization in childhood in a cohort study. Pediatr Allergy Immunol. 2014 Oct;25(6):565-71
3. Silva RA, Almeida FM, Olivo CR, Saraiva-Romanholo BM, Martins MA, Carvalho CR. Airway remodeling is reversed by aerobic training in a murine model of chronic asthma. Scand J Med Sci Sports. 2015 Jun;25(3):e258-66
4. Han L, Wang L, Tang S, Yuan L, Wu S, Du X, Xiang Y, Qu X, Liu H, Luo H, Qin X, Liu C. ITGB4 deficiency in bronchial epithelial cells directs airway inflammation and bipolar disorder-related behavior. J Neuroinflammation. 2018 Aug 31;15(1):246
5. Sachdeva K, Do DC, Zhang Y, Hu X, Chen J, Gao P. Environmental Exposures and Asthma Development: Autophagy, Mitophagy, and Cellular Senescence. Front Immunol. 2019 Nov 29;10:2787
6. Qin Q, Chen X, Feng J, Qin L, Hu C. Low-intensity aerobic exercise training attenuates airway inflammation and remodeling in a rat model of steroid-resistant asthma. Chin Med J (Engl). 2014;127(17):3058-64

7. Tan M, Liu C, Huang W, Deng L, Qin X, Xiang Y. CTNNAL1 inhibits ozone-induced epithelial-mesenchymal transition in human bronchial epithelial cells. Exp Physiol. 2018 Aug;103(8):1157-1169
8. Giannella M, Valerio M, Franco JA, Marin M, Bouza E, Muñoz P. Pacemaker infection due to Mycobacterium fortuitum: the role of universal 16S rRNA gene PCR and sequencing. Diagn Microbiol Infect Dis. 2007 Mar;57(3):337-9
9. Erb-Downward JR, Thompson DL, Han MK, Freeman CM, McCloskey L, Schmidt LA, Young VB, Toews GB, Curtis JL, Sundaram B, Martinez FJ, Huffnagle GB. Analysis of the lung microbiome in the "healthy" smoker and in COPD. PLoS One. 2011 Feb 22;6(2):e16384
10. O'Dwyer DN, Ashley SL, Gurczynski SJ, Xia M, Wilke C, Falkowski NR, Norman KC, Arnold KB, Huffnagle GB, Salisbury ML, Han MK, Flaherty KR, White ES, Martinez FJ, Erb-Downward JR, Murray S, Moore BB, Dickson RP. Lung Microbiota Contribute to Pulmonary Inflammation and Disease Progression in Pulmonary Fibrosis. Am J Respir Crit Care Med. 2019 May 1;199(9):1127-1138
11. Huang YJ, Erb-Downward JR, Dickson RP, Curtis JL, Huffnagle GB, Han MK. Understanding the role of the microbiome in chronic obstructive pulmonary disease: principles, challenges, and future directions. Transl Res. 2017 Jan;179:71-83
12. Garcia-Nuñez M, Millares L, Pomares X, Ferrari R, Pérez-Brocal V, Gallego M, Espasa M, Moya A, Monsó E. Severity-related changes of bronchial microbiome in chronic obstructive pulmonary disease. J Clin Microbiol. 2014;52(12):4217-23.
13. Huang YJ, Sethi S, Murphy T, Nariya S, Boushey HA, Lynch SV. Airway microbiome dynamics in exacerbations of chronic obstructive pulmonary disease. J Clin Microbiol. 2014;52(8):2813-23.
14. Timm J, Post FA, Bekker LG, Walther GB, Wainwright HC, Manganelli R, Chan WT, Tsenova L, Gold B, Smith I, Kaplan G, McKinney JD. Differential expression of iron-, carbon-, and oxygen-responsive mycobacterial genes in the lungs of chronically infected mice and tuberculosis patients. Proc Natl Acad Sci USA. 2003;100:14321-6
15. Qiu X, Ye Q, Sun M, Wang L, Tan Y, Wu G. Saturated hydrogen improves lipid metabolism disorders and dysbacteriosis induced by a high-fat diet. Exp Biol Med (Maywood). 2020 Jan 7:1535370219898407
16. Ohno K, Ito M, Ichihara M. Molecular hydrogen as an emerging therapeutic medical gas for neurodegenerative and other diseases. Oxid Med Cell Longev. 2012;2012:3531-52
17. Ohsawa I, Ishikawa M, Takahashi K, Watanabe M, Nishimaki K, Yamagata K, Katsura K, Katayama Y, Asoh S, Ohta S. Hydrogen acts as a therapeutic antioxidant by selectively reducing cytotoxic oxygen radicals. Nat Med. 2007;13:688-94
18. Kamimura N, Nishimaki K, Ohsawa I, Ohta S. Molecular hydrogen improves obesity and diabetes by inducing hepatic FGF21 and stimulating energy metabolism in db/db mice. Obesity (Silver Spring). 2011;19:1396-403
19. Song G, Lin Q, Zhao H, Liu M, Ye F, Sun Y, Yu Y, Guo S, Jiao P, Wu Y, Ding G, Xiao Q, Qin S. Hydrogen activates ATP-binding cassette transporter A1-dependent efflux ex vivo and improves high-density

lipoprotein function in patients with hypercholesterolemia: a double-blinded, randomized, and placebo-controlled ttrial. J Clin Endocrinol Metab. 2015;100:2724-33

20. Li L, Liu M, Kang L, Li Y, Dai Z, Wang B, Liu S, Chen L, Tan Y, Wu G. HHEX: A crosstalker between HCMV infection and proliferation of VSMCs. Front Cell Infect Microbiol. 2016;6:169
21. Silva FMCE et al. High-fat diet-induced obesity worsens TH2 immune response and immunopathologic charactersitics in murine model of eosinophilic oesophagitis. Clin Exp Allergy. 2020
22. Mayor RS, et al. Maternal high-fat-diet is associated with impaired fetal lung development. Am J Physiol Lung Cell Mol Physiol. 2015
23. Ha S1, Shin B1, Park W. Lack of glyoxylate shunt dysregulates iron homeostasis in Pseudomonas aeruginosa. Microbiology. 2018 Apr;164(4):587-599
24. Lorenz MC, Bender JA, Fink GR. Transcriptional response of Candida albicans upon internalization by macrophages. Eukaryot Cell. 2004; 3: 1076-1087
25. McKinney JD, Honer zu Bentrup K, Munoz-Elias EJ, et al. Persistence of Mycobacterium tuberculosis in macrophages and mice requires the glyxylate shunt enzyme isocitrate lyase. Nature. 2000; 406: 735-738
26. Honer Zu Bentrup K, Miczak A, Swenson DL, et al. Characterization of activity and expression of isocitrate lyase in Mycobacterium avium and Mycobacterium tuberculosis. J Bacteriol. 1999; 18: 7161-7167
27. Hamilton AJ, Jeavons L, Youngchim S, et al. Sialic acid-dependent recognition of laminin by Penicillium marneffei codidia. Infect Immun. 1998; 66: 6024-6026

Figures

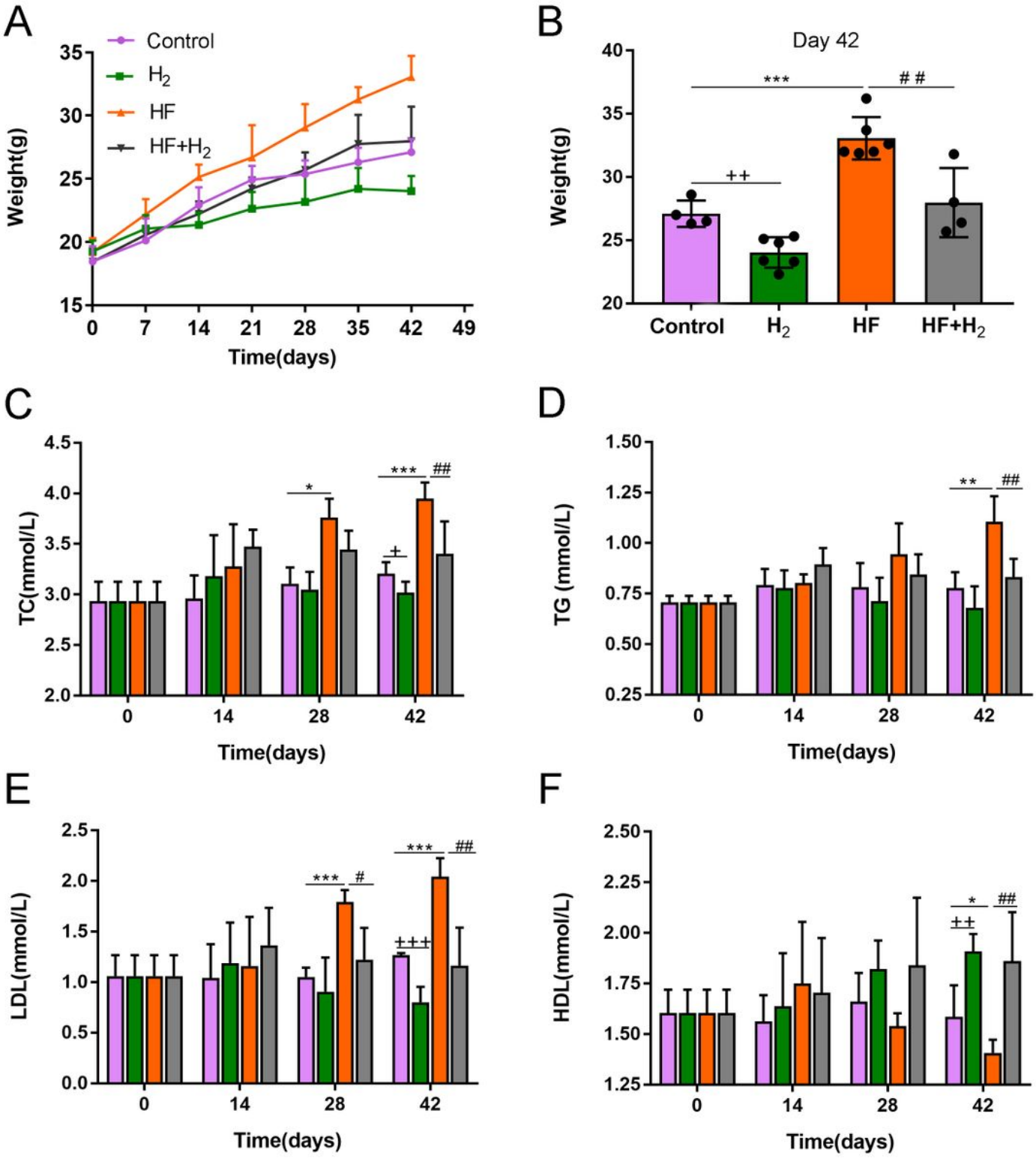

Figure 1

Saturated hydrogen inhibits the increase in body weights and improves dyslipidemia induced by a high-fat diet (n = 6). A, Changes of weight with time. B, Weight of mice on day 42. C- F represented the changes of TC, TG, LDL and HDL in peripheral blood of mice with time. (* $p < 0.05$, ** $p < 0.01$ and *** $p < 0.001$ vs. Control; + $p < 0.05$, ++ $p < 0.01$ and +++ $p < 0.001$ vs. Control; # $p < 0.05$ and ## $p < 0.01$ vs. HF.)

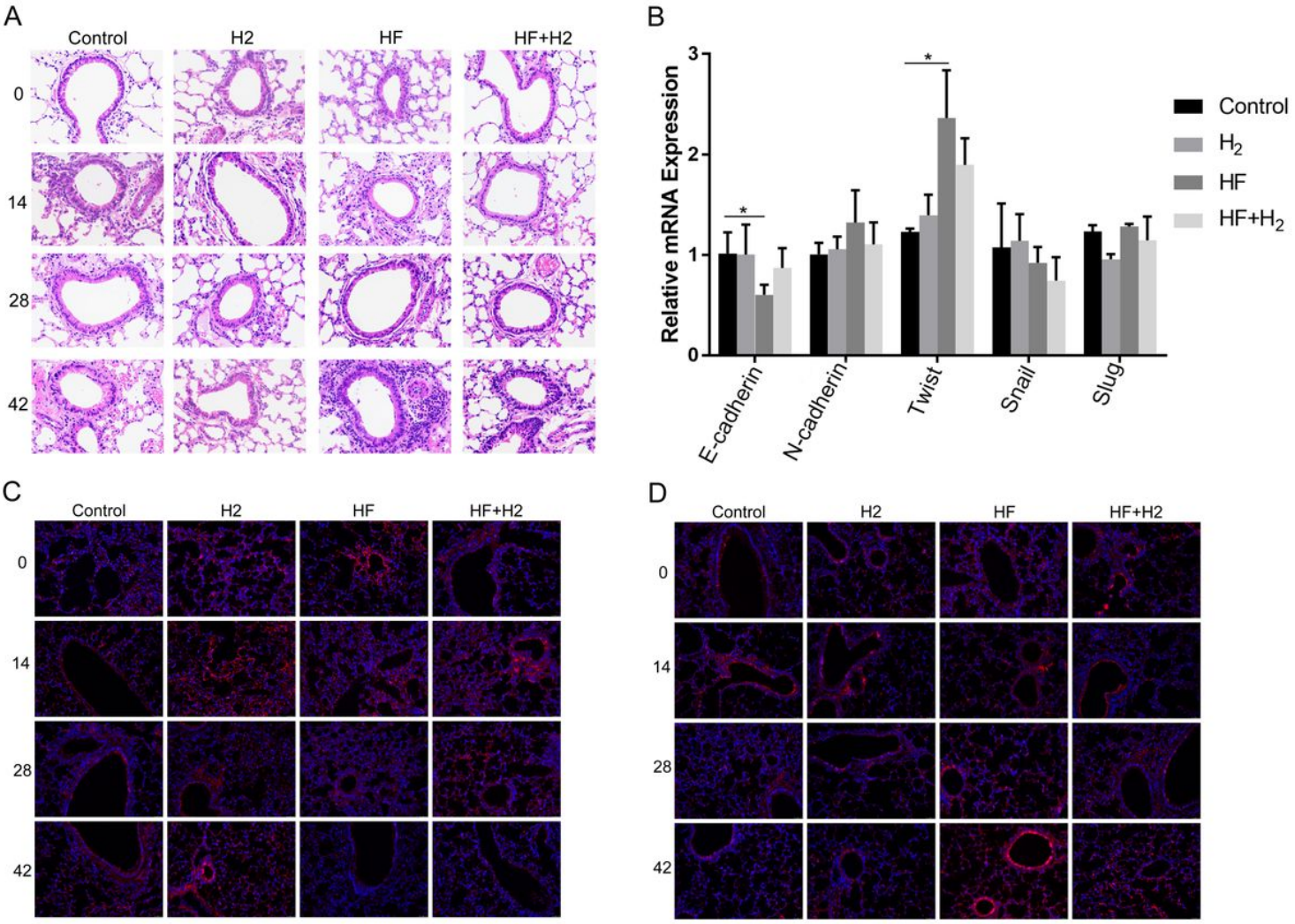

Figure 2

Changes of lung tissue related indexes of mice in each group (n = 6). A, HE staining of lung tissues. B showed the expression of E-cad, N-cad, twist, snail and slug mRNA in lung tissues on day 42 using qPCR C, Immunofluorescence of E-cad protein in lung tissues. D, Immunofluorescence of twist protein in lung tissues. (* $p < 0.05$ vs. Control.)

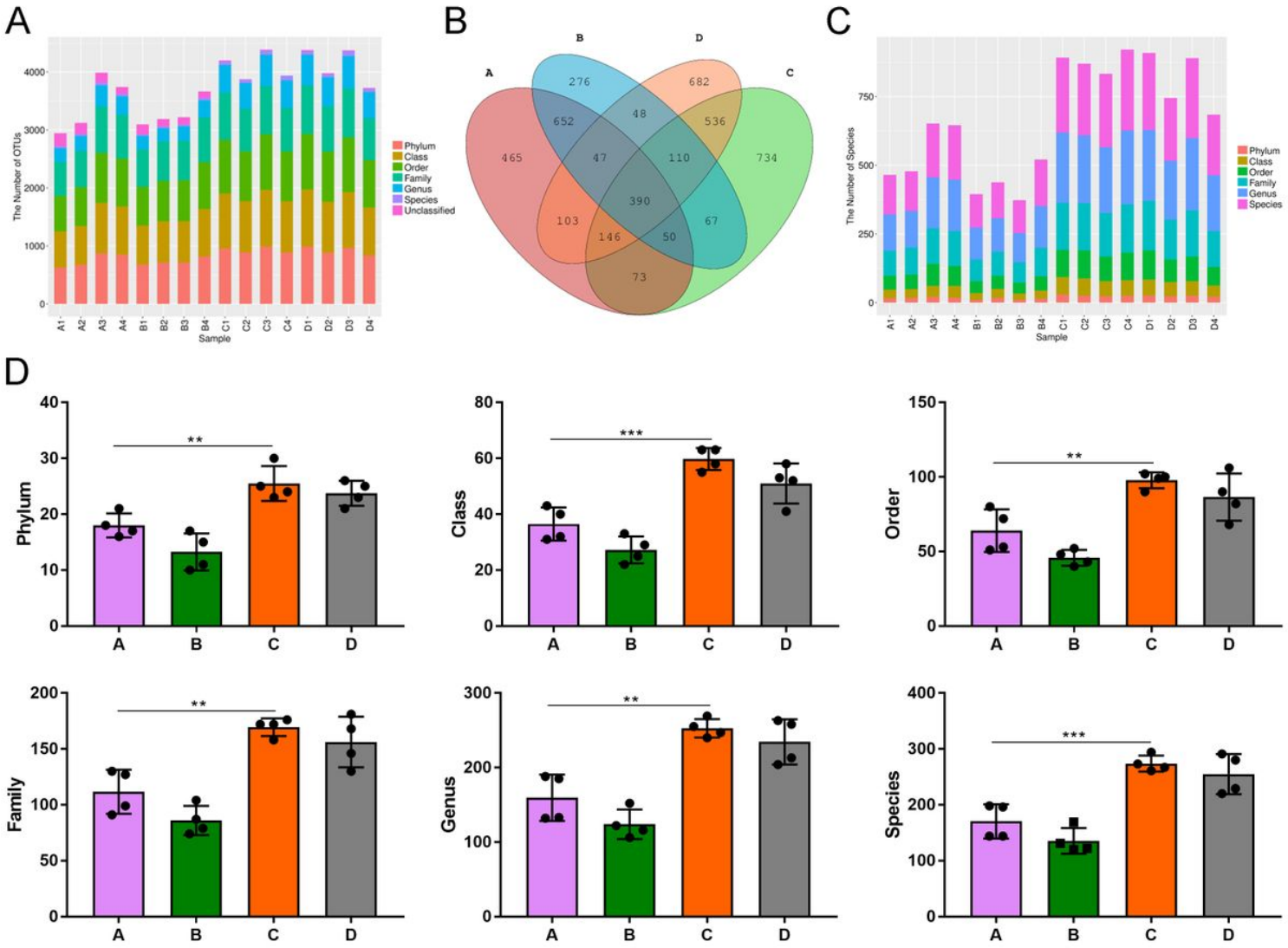

Figure 3

OTU partition and distribution in each group. A: Statistical chart of OTU classification and classification status identification results. The abscissa is arranged according to the sample name, and the ordinate is the number of OTU in each sample that can be classified to each classification level of phylum, class, order, family, genus and species. B: Venn diagram. Each ellipse represents a group of samples. The overlapping area between ellipses indicates the shared OTUs between groups. The number of each block indicates the number of shared or unique OTUs contained in the block. C: Statistical chart of microbial groups at each classification level. The abscissa is arranged according to the sample name, and the ordinate is the number of microbial groups of each sample at the classification level of phylum, class, order, family, genus and species. D: The statistical chart of the microbial groups in each group at the classification level of phylum, class, order, family, genus and species. (** $p < 0.01$ and *** $p < 0.001$ vs. Control.)

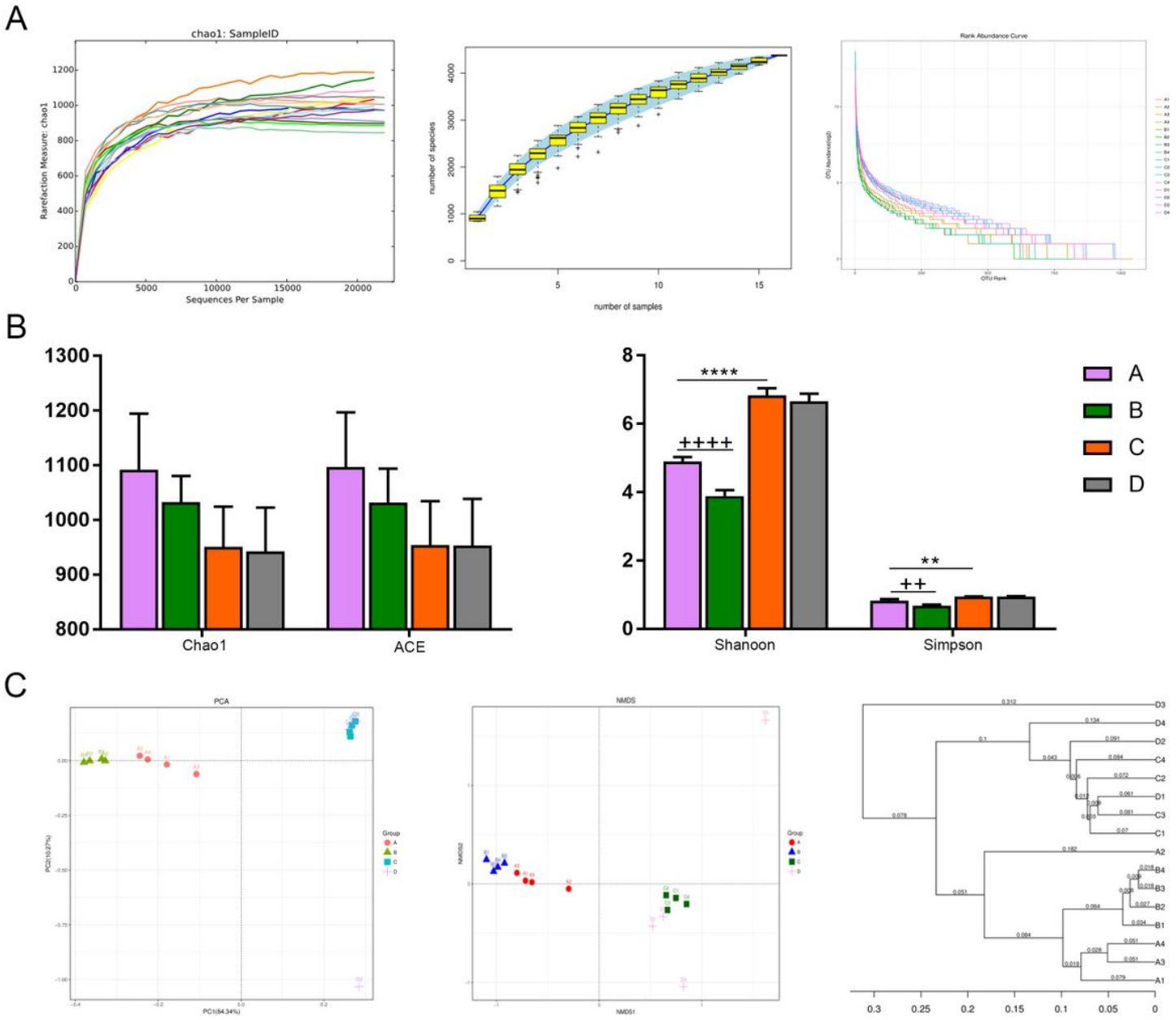

Figure 4

Sequencing quality and microecological diversity analysis of lung in each group. A Rarefaction sparse curve, Specaccum species accumulation curve and abundance rank curve for Alpha diversity analysis are presented. B, There are Alpha diversity index (microbial diversity index) Chao1, ACE, Shannon and Simpson statistical charts in order. C, It is the principal component analysis graph (PCA), multidimensional scale analysis graph (MDS) and sample clustering analysis graph (UPGMA) of Beta diversity analysis. (** $p < 0.01$ and **** $p < 0.0001$ vs. Control; ++ $p < 0.01$ and ++++ $p < 0.0001$ vs. Control.)

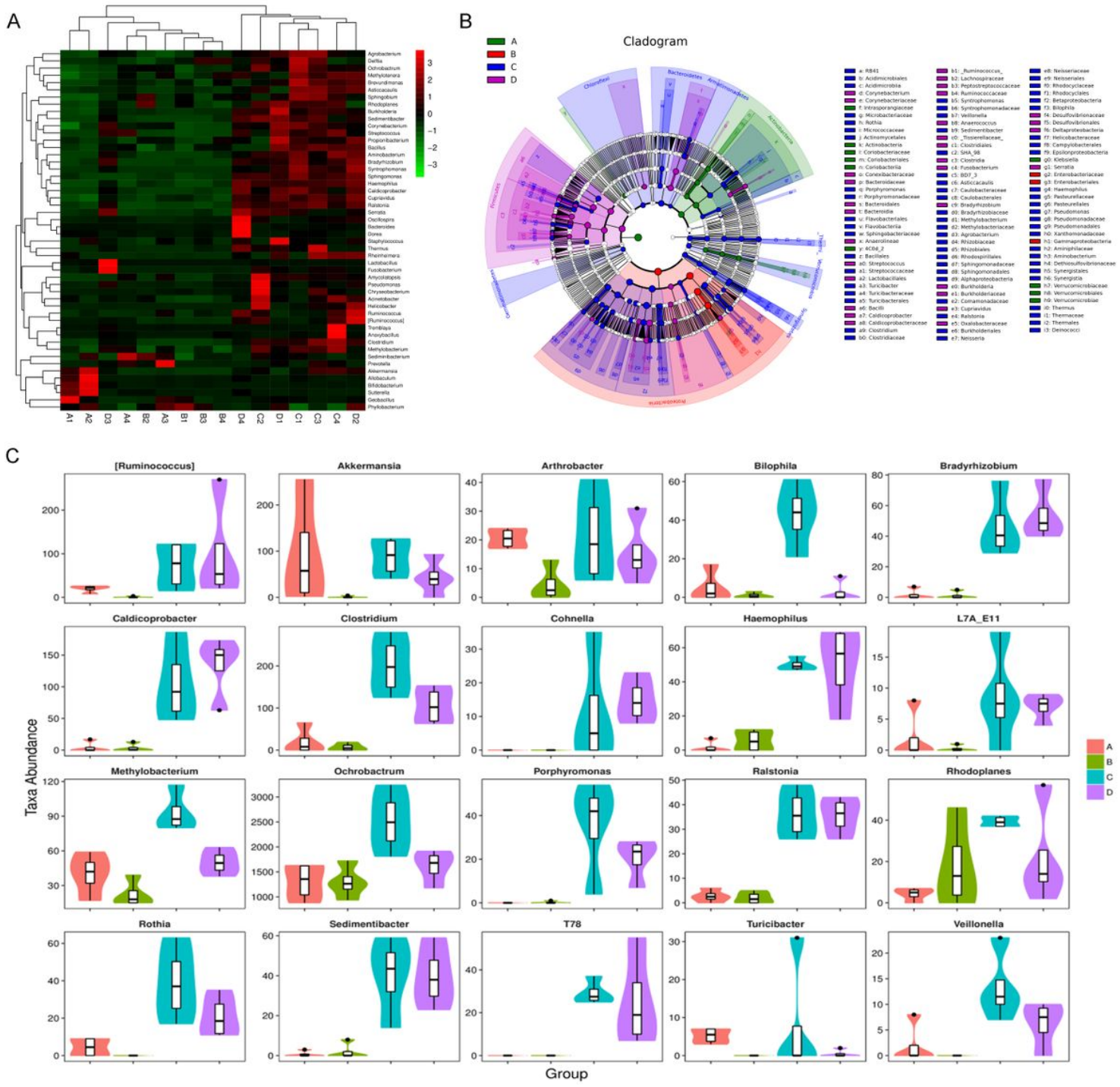

Figure 5

The difference analysis of microflora in the lung of each group and the identification of key microbes. A, at the genus level, cluster analysis of the top 50 bacteria in each sample. Samples were first clustered based on their similarity, and then arranged horizontally according to the clustering results. The taxa are also clustered according to the similarity of their distribution in different samples and arranged vertically according to the clustering results. In figure A, red represents the genus with higher abundance in the corresponding sample, while green represents the genus with lower abundance. B, Cluster analysis diagram of taxa with significant differences among groups. From the inner circle to the outer circle are

phylum, class, order, family, and genus. The fan area represents the abundance of bacteria. C, The abundance of the first 20 taxa with the most significant differences in each group. In the figure, the abscissa is the first 20 taxon with the most significant difference, and the ordinate is the sequence quantity of each taxon in various groups. The "fat and thin" of "violin" reflects the density of sample data distribution, and the wider the width, the more samples corresponding to this sequence quantity. The border of the boxplot represents the Interquartile range (IQR), the horizontal line represents the median value, the upper and lower tentacles represent the IQR range of 1.5 times beyond the upper and lower quartile, and the symbol "•" represents the extreme value beyond the range.

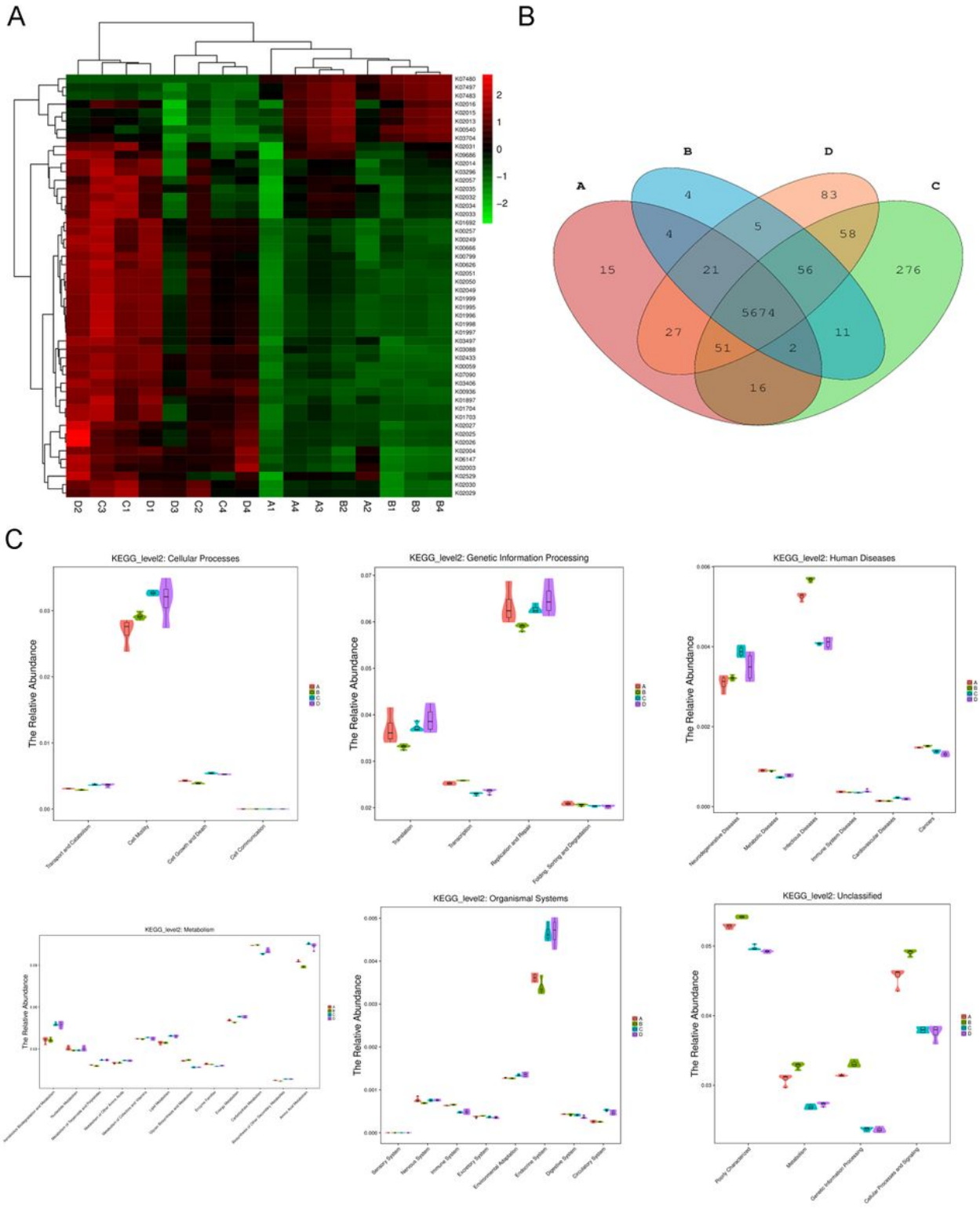

Figure 6

Prediction of microbial metabolism. A, The heat map of clustering analysis of functional groups in the first 50 abundances. The samples were first clustered according to the similarity of the abundance distribution of functional groups, and then arranged horizontally based on the clustering results. Functional groups are also clustered according to the similarity of their distribution in different samples, and arranged vertically according to the clustering results. In the figure, red represents the functional

group with higher abundance in the corresponding sample, while green represents the functional group with lower abundance. B, Venn diagram. Each ellipse represents a set of samples. The overlapping regions between the ellipses indicate the common functional groups among each group, and the number of each block indicates the number of common or unique functional groups contained in the block. C, Analysis diagram of KEGG database for prediction of microbial metabolism function. In the figure, the abscissa is the second functional group of KEGG, and the ordinate is the relative abundance of each functional group in each group. The "fat and thin" of the "violin" reflects the density of the distribution of sample data. The wider the width, the more samples there are under this abundance. The border of the boxplot represents the Interquartile range (IQR), the horizontal line represents the median value, the upper and lower tentacles represent the IQR range of 1.5 times beyond the upper and lower quartile, and the symbol "•" represents the extreme value beyond the range.

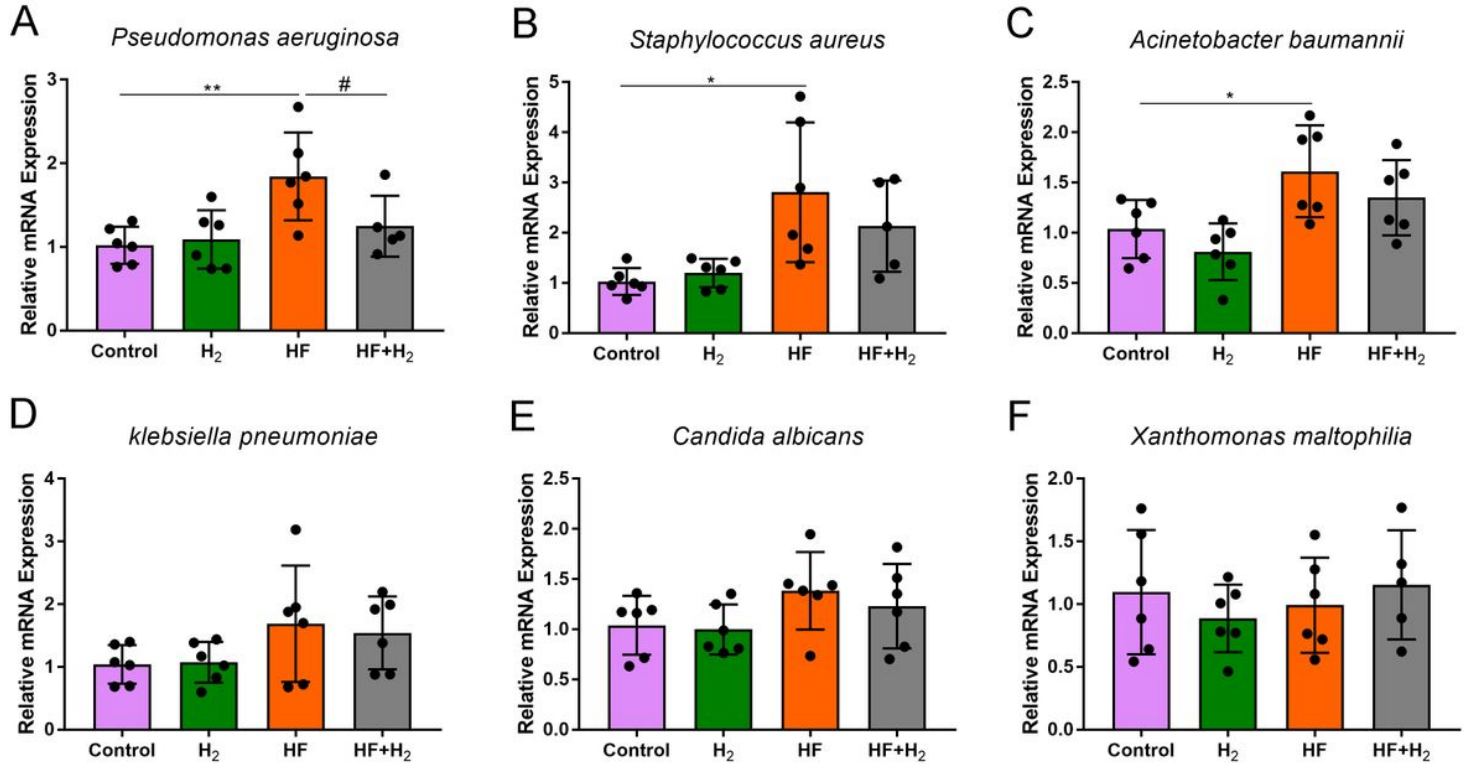

Figure 7

Changes in the expression of ICL genes in several bacteria or fungi significantly associated with respiratory disease (n = 6). A-F was the ICL expression level of P. aeruginosa, S. aureus, A. baumannii, K. pneumoniae, C. albicans and X. maltophilia in the lung tissues of each group detected by qPCR. (* $p < 0.05$ and ** $p < 0.01$ vs. Control; # $p < 0.05$ vs. HF.)

Supplementary Files

This is a list of supplementary files associated with this preprint. Click to download.

- Supplementarymaterials.docx